ISSN (Online): 2583-7052

International Journal of Advanced Trends in Engineering and Management (IJATEM)
Vol. 03 (10), October 2024, pp. 16-30

Article Title: An Efficient Framework for Lung Cancer Prediction Using LBP Extraction and Cascaded CNN

An Efficient Framework for Lung Cancer Prediction Using LBP Extraction and Cascaded CNN

P. Lavanya

Research scholar, Department of Electronics and Communication Engineering, Saveetha School of Engineering, Saveetha Institute of Medical and Technical Sciences, Chennai - 602105, Tamil Nadu, India. plavanyame@gmail.com

ABSTRACT

Lung cancer, which affects both men and women, is currently the leading cause of cancer-related fatalities globally. Lung cancer is mostly caused by smoking. It is thought that 90% to 95% of cases of lung cancer begin in the epithelial cells lining the bigger and smaller airways (bronchi and bronchioles), while the illness can grow elsewhere in the lung. Medical responsibilities make a better treatment decision for patient diagnosis and treatment to find a lung cancer at early stage using the classification models. This study's main goal is to identify lung cancer by employing Cascaded Convolutional Neural Networks (CNN) with Local Binary Pattern and Wiener Filter. The lung image dataset is taken as the input. The lung images have been pre-processed by Wiener filter. After, the processed images are segmented using the Otsu Binary Threshold method. The features of the cancer-affected images are to be extracted using the Local Binary Pattern approach. This work implements in a python platform for developing a classification of lung images using the Cascaded CNN classifier. The proposed Cascaded CNN technique provides more accuracy than other classification models for predicting lung cancer. The proposed classifier shows the highest specificity 95% of and sensitivity of 94%.
Keywords: Wiener Filter, Otsu Binary Thresholding, Local Binary Pattern, Cascaded CNN

1 Introduction

The most common cause of cancer-related death globally is lung cancer, and many patients receive a diagnosis at an advanced stage. For early detection, the most recent and advanced technique is computed tomography (CT) screening [1]. Dual-modality medical imaging devices called Positron Emission Tomography/Computerized Tomography (PET/CT) systems gather anatomical and metabolic data for analysis [2].Appropriate treatment for lung cancer patient is mostly determined by the type of lung cancer, such as non-small cell lung cancer (85%) or small cell lung cancer (15%). The most prevalent non-small cell lung cancer is classified into a number of subgroups, including squamous cell carcinomas (SCs) and adenocarcinomas (ADCs), which are named after the tumor cells [3]. Early lung cancer identification improves the chance of a successful diagnosis and prompt treatment, which raises the patient survival rate. Accurately locating the malignancy is necessary for chemotherapy, the primary treatment for lung cancer. To ascertain the stage of cancer, accurate volume estimation is required [4]. Early cancer identification is crucial, but the available methods are insufficient. Even though imaging-based pathological diagnosis has a high degree of accuracy, it can only be used once the tumor has reached a specific size. In order to make accurate treatment decisions, both patients and doctors need quantitative data regarding potential benefits of a cancer treatment [5]. The computer software provides such information. Tools to assist doctors in integrating prognostic data for cancer patients are required. These methods improve prognostic estimation accuracy and consistency and help determine whether treatments are worthwhile to pursue in standard clinical practice. To create decision support systems for identifying lung cancer, image characteristics from a complete lung image are extracted and analysed [6]. Based on patient records, the clinicians utilize machine learning techniques to help them make better treatment decisions. The two types of cutting-edge lung nodule identification systems are those based on deep learning and others based on traditional machine learning [7].

Before entering the feature description into the classifier for lung nodule detection, the features are first manually extracted. The deep learning approach is implemented on a computer-assisted detection system that uses neural networks that self-learn to automatically extract information in order to identify lung nodules [8]. Numerous machine learning techniques are employed to determine the size, features, and presence of malignancy in nodules. Numerous novel methods were created to enhance neural network training [9-10].Lung cancer patients have an extremely low long-term endurance rate when compared to patients with other cancer types. Therefore, early detection of lung cancer is crucial and offers an essential research platform in the field of medical image processing [11-13]. In order to predict lung cancer, image processing techniques are important. Several classification methods are used to predict lung cancer. These include the Random Forest classifier, KNN, Decision Trees, Support Vector Machines (SVM), and Artificial Neural Networks (ANN). Using this method, the CT image is preprocessed, the lung region is segmented, the features of the discovered lung nodule are extracted, and the nodules are classified [14-15].

This study uses cascaded CNN with LBP to present a thorough and comparative approach for detecting lung cancer in CT scan pictures. In order to filter the image and eliminate noise, the wiener filter is used for preprocessing. To segment the image, the Otsu Binary Threshold technique is employed. The goal of developing this type of structure is to identify the kind of feature extractor and learning strategy that yield the most precise detection system. As a result, there are fewer false positives and a higher detection accuracy for lung cancer. Experiments show that our suggested model performs noticeably better than current lung tumor detectors when the suggested lung-cancer detection method is tested against established benchmarks.

2 Related Works

Mahmoud Ragab et al. (2023) [16] have presented a technique called SCMO-MLL2C and it is a lung cancer classification method for self-upgraded cat mouse using CT scans. Gaussian

International Journal of Advanced Trends in Engineering and Management (IJATEM)
Vol. 03 (10), October 2024, pp. 16-30

filtering (GF) is the method used by the SCMO-MLL2C technique to denoising the images. Additionally, the slime mold algorithm (SMA) is used in the feature extraction process using densely linked networks (DenseNet-201). Using the Elman Neural Network (ENN) approach, lung cancer was classified. This model only works with a limited number of datasets in a certain image format.

Vani Rajasekar et al. (2023) [17] have presented a Convolution Neural Network (CNN), CNN Gradient Descent (CNN GD), VGG-16, VGG-19, Inception V3 and Resnet-50 algorithms for evaluating the performance in deep learning. The evaluation of the results demonstrates that, the detection accuracy improved at the analysis of histopathological tissues. Moreover, the performance of the model across diverse datasets and medical scenarios remains unexplored, as does its evaluation on larger datasets to ascertain applicability and robustness.

Tehnan I. A. Mohamed et al. (2024) [18] have developed a novel method for predict lung cancer by combining DNA methylation, miRNA, and mRNA indicators. The synthetic minority over-sampling method (SMOTE) approach is used to guarantee class balance, and principal components analysis (PCA) is used to modernized features. Following integration and processing, the data is fed into the PCA-SMOTE-CNN classification method. However, this work is unpredictable for multi-omics data in a number of fascinating directions.

Rabbia Mahum et al (2023) [19] have proposed a lung tumor detection method, called Lung-RetinaNet. In order to increase the shallow prediction layer perceptive information, a multi-scale feature module is introduced to combining the layers of network. Additionally, the context module uses a streamlined and lightweight method to enhance features and locate the small tumors efficiently. Furthermore, this model takes a long time to train the dataset.

Muhammad Imran et al (2024) [20] have focused on developing a novel deep-learning architecture that combines vision transformers (ViTs) and convolutional neural networks (CNNs) in order to improve the accuracy in classification of non-small cell lung cancer (NSCLC) histopathology pictures. While ViTs are used to comprehend long-range correlations between picture patches, CNNs are utilized to capture local features. Concentrating on its potential for actual applications where speed and accuracy are low.

3 Proposed Work

This method first pre-processes the input lung image dataset by applying a wiener filter to reduce noise and improve picture quality. After preprocessing, the image segments and pixels are segmented using the Otsu Binary Threshold segmentation technique. In the feature extraction process, the dataset's texture information is encoded and features are extracted using the Local Binay Pattern (LBP) approach. Lung images are classified and lung cancer is detected using a cascaded convolutional neural network. Python platform is used for implementing the prediction model. Furthermore, a performance matrix module computes metrics including accuracy, precision, F1-score, and recall value to assess the model's effectiveness. Figure 1

International Journal of Advanced Trends in Engineering and Management (IJATEM)
Vol. 03 (10), October 2024, pp. 16-30

Article Title: An Efficient Framework for Lung Cancer Prediction Using LBP Extraction and Cascaded CNN

shows the procedures used for lung cancer prediction using the Cascaded Convolutional Neural Network classification model.

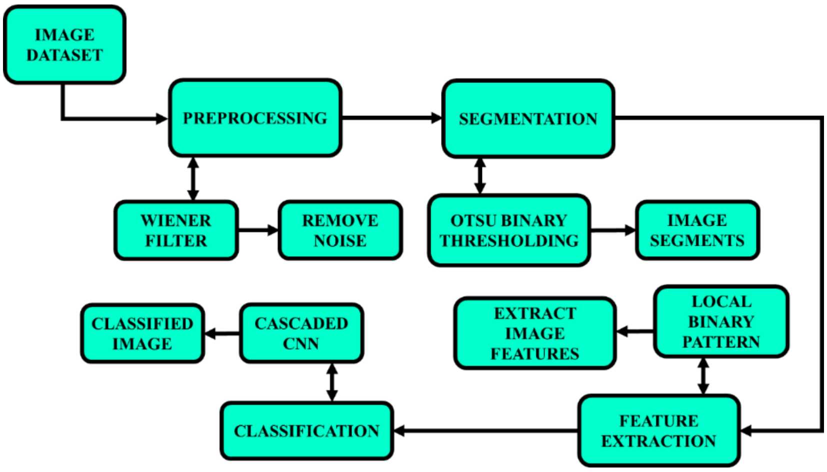

Figure 1: Block Diagram for proposed system

3.1 Image Preprocessing By Wiener Filter

For predicting lung cancer, a collection of actual patient CT scan image is retrieved from the Lung Image Database .Initially, the lung image data are pre-processed using the preprocessing technique to filter the image and removes speckle noise. Pre-processing is the process of improving image data by reducing undesirable distortions or enhancing certain aspects of the image that are important for tasks related to further processing and analysis. Outlier detection, missing value treatments, and removing undesirable or noisy data are a few examples of image pre-processing. In the context of cancer imaging, image preprocessing is the collection of procedures used on unprocessed medical images to improve their quality, standardize their format, and get them ready for additional examination. This prepares the image for segmentation, feature extraction and classification. Variety of filtering techniques apply to remove the unwanted noise from the images. To eliminate noise from the input lung imaging dataset, the Weiner Filter approach is suggested.

Digital image development is the primary use for the Weiner filter. In order to decrease noise, the de-convolution approach frequently employs linear invariant methods. Additionally, the Weiner filter reduces the Mean Square Effect (MSE) between the image's intended and estimated blur signals. Based on statistics gathered from each pixel's local neighborhood, the Wiener filter is used to remove noise from a detected deformed image. The benefit of applying the Weiner filter is that, in addition to lowering blur, it also lowers any remaining noise in the denoised image, which slightly improves the visual quality of the image.

The algorithmic procedures of the Weiner Filter is performed as follows: The lung image dataset is taken for preprocessing. In the preprocessing step, initially the Weiner filter read the image and convert the input image into gray scale image. By redistributing the gray value employed, this technique increases the visibility of the image hidden features.

ISSN (Online): 2583-7052

International Journal of Advanced Trends in Engineering and Management (IJATEM)
Vol. 03 (10), October 2024, pp. 16-30

Article Title: An Efficient Framework for Lung Cancer Prediction Using LBP Extraction and Cascaded CNN

Q (N×N) = image, P (i, j) = pixel range, Q (N×N) → R (N×N).

$$P_n = 255\left(\frac{|\varphi w(P)-\varphi w(min)|}{|\varphi(max)-\varphi w(min)|}\right) \quad (1)$$

$$\varphi w(P) = \left[1 + \exp\left(\frac{\mu w - p}{\sigma w}\right)^{-1}\right] \quad (2)$$

$$(u,v) = \left(\frac{H^*(u.v)Ps(u,v)}{|H(u,v)|^2 Ps(u,v)+Pn(u,v)}\right. \quad (3)$$

$$G(u,v) = \left(\frac{H^*(u,v)}{|u,v|^2+\frac{Pn(u,v)}{Ps(u,v)}}\right) \quad (4)$$

(u, v) = degradation role, $H^*(u,v)$ = conjugate function of complex decomposition, Pn(u, v) = Energy Density in noise spectral, Ps(u, v) = Image Density

The enhanced image is shown based on equation (3) and (4) after the Weiner filter is applied, and the visual quality of the lung image also improved. The segmentation technique will be used with this denoising image.

3.2 Segmentation by Otsu Binary Threshold

Segmenting images divide a digital image into several parts (objects or regions) in order to simplify and analyze the image by dividing it into relevant parts. A collection of segments that together include the full image is the ultimate result of image segmentation. A region's pixels are all comparable in terms of a computed feature or characteristic, such color, texture, or intensity. This approach makes use of threshold-based segmentation. This method looks for related pixels by identifying peak values in the image's histogram. It is a straightforward procedure that doesn't require complex pre-processing.

Otsu Binary Threshold technique is proposed for segmenting lung images after preprocessing. This is the simplest technique for segmenting images. Otsu's approach uses binary images and automatically applies clustering-based image thresholding. It is also employed to detect any defects in the image. Segmentation is carried out iteratively using threshold values. Every time a new threshold is calculated, the highest variance is used to determine the intended threshold. A grayscale image denoted by k is searched for the threshold value. Equation (5) displayed the probability of every pixel at the i level.

k = 1, 2………,L, L=255

$$p(i) = \frac{n_i}{N}, p(i) \geq 0, \sum_1^{256} p(i) = 1 \quad (5)$$

n_i = number of pixels in i, N = image pixels

The weight values of object and background classes are calculated as $w_1$andw_2. $m_1$and $m_2$are the mean values of both classes. Equations (6) and (7) are used to find the average of the two classes.

$$m_1(t) = \sum_{i=1}^{t} i.p(i)/w_1(t) \quad (6)$$

$$m_2(t) = \sum_{i=1}^{t} i.p(i)/w_2(t) \tag{7}$$

The probability is always I which is displays in equation (8).

$$w_1(t) + w_2(t) = 1 \tag{8}$$

The between -class variance (BSV) is shown in equation (9).

$$\sigma b^2(t) = w_1.[m_1(t) - m_T]^2 + w_2.[m_2(t) - m_T]^2 \tag{9}$$

$$t = \max\{\sigma b^2(t)\} \tag{10}$$

Equation (10), which displays the highest between-class variance (BCV), is the most suitable thresholding value of Otsu. The lung images are segmented according to the variance value. The threshold is automatically fixed, segmentation is carried out, and the outcome is generated. This approach yields extremely accurate and obvious results. The segmented image is used to extract features.

3.3 Feature Extraction by Local Binary Pattern

In image processing, feature extraction is the process of locating and displaying unique structures in an image. This procedure converts unprocessed visual input into numerical characteristics while maintaining the most important details. Shape based feature extraction, transform based features, local feature descriptors, local binary pattern, local decimal pattern and revolutionized automated feature extraction are the various kinds of feature extraction algorithms used for feature extraction in digital images. To extract the features from the lung images, the Local Binary Pattern (LBP) extraction method is suggested. By transforming an image pixel value to a binary value depending on the value of its neighboring pixels, this approach extracts the texture features.

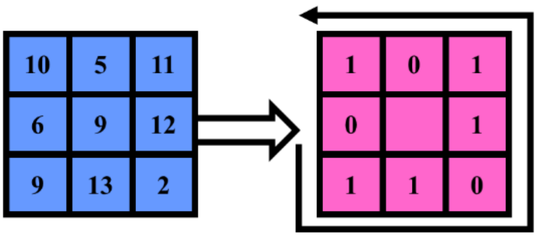

Figure 2: 3×3 matrix LBP computation

Figure 2 indicates the matrix representation of LBP computation to get a binary values. Using the LBP algorithm, a 3x3 pixel image fragment is taken, and the binary pattern is then calculated by using the pixel in the center and its neighboring pixels. The following formula is used to determine the binary pattern.

$$LBP_{(p,r)} = \sum_{p=0}^{p-1} s(g_p - g_c)2^p, \; s(x) = \begin{Bmatrix} 1, x \geq 0 \\ 0, x < 0 \end{Bmatrix} \tag{11}$$

International Journal of Advanced Trends in Engineering and Management (IJATEM)
Vol. 03 (10), October 2024, pp. 16-30

Two parameters are taken from equation (11) in order to complete the computation using LBP. The two parameters are the number of neighbors, denoted by variable p, and the pixel radius, indicated by variable r. The variable g_c represents the value of the central pixel and the value of the neighboring pixel. The function s process the subtraction result of $g_p$with g_c. The s function returns 0 if the subtraction result is less than 0 and 1 if the subtraction result is equal to or greater than 0. The thresholding values are computed according to equation (11). Finally it provides the LBP for the image. After extracting the features of the lung images using the LBP feature extractor, the results are used for classifying the images.

3.4 Classification Using Cascaded CNN

Classifying every pixel in a digital image into one of several classes is the primary objective of the classification process. This classification algorithms build a classifier to classifying the images. This work proposed cascaded convolutional neural networks (CNNs) to analyze pixel-level details, identifying patterns that teach models about the real world. Both supervised and unsupervised image classification methods frequently use CNNs, which automatically extract hierarchical features from images. This enhances the data labelling accuracy and refines the image search methods.

Cascaded CNN is the best tool for image detection and classification. The binary classification problem is used to train the classification network. For two classes, the classification network's output is expressed in terms of probability. A limited number of processing layers make up a deep CNN model, which learns different aspects of the input image. The Cascaded CNN architecture includes Dense layers for classification. The deeper layers learn and extract the low level features of image, while the initiatory layers learn and extract the high level features. The weight sharing feature of CNN lowers the number of trainable parameters in the network, is one of the primary justifications for taking the network into consideration in this instance. In addition to improving generality, it prevents overfitting. The description of a CNN is displayed as follows:

$$x^1 \to w^1 \to x^2 \to \cdots \to w^{L-1} \to x^L \to w^L \to z \quad (12)$$

A CNN progresses in a layer-by-layer fashion, as indicated by equation (12). The input value'x^1', is processed by w^1(together referred to as a tensor) in the first layer. This layer are potentially a fully connected layer, pooling layer, convolutional layer, etc. The procedure keeps going until the (L-1) th layer is reached, which is typically a loss layer after a softmax layer (to createx^L a probability mass function).Figure 3 illustrates the layers in the cascaded CNN classifier structure.

International Journal of Advanced Trends in Engineering and Management (IJATEM)
Vol. 03 (10), October 2024, pp. 16-30

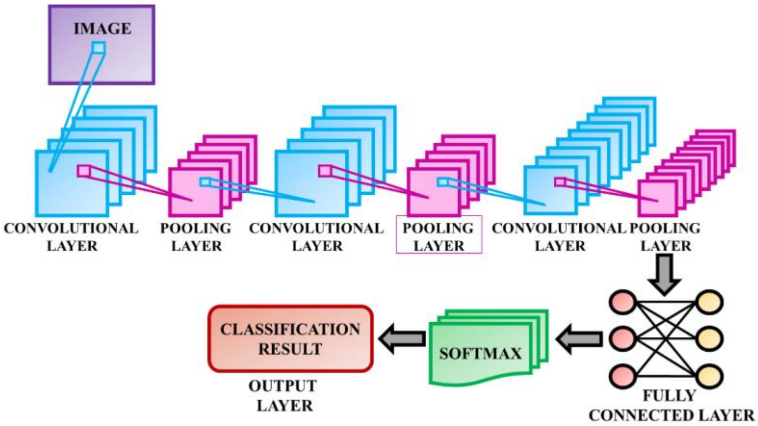

Figure 3: Structure of Cascaded CNN

First, the networks with image datasets are subjected to transfer learning. Assessing the cancer prediction rate on lung images comes subsequently. Furthermore, this model calculates the probability that x^1 will subsequently represent C categories. Thus, the output is the Cascaded CNN predictions. The mathematical expression for the convolutional process is:
x^L€ R C = column vector with C elements

$$y_{i^{l+1},j^{l+1},d} = \sum_{i=0}^{H} \sum_{j=0}^{W} \sum_{d^l}^{D^l} f_{i,j,d^l,d} \times x^l\, i^{l+1} + i, j^{l+1} + j, d^l \tag{13}$$

x = tensor of third order, H, W, D = elements of index-triplet (i,j,d), X € R.

$$0 \leq d \leq D = D^{l+1} \tag{14}$$

Because every location in the space has the same filter, fewer parameters are used, which decreases the training time. This is what makes CNNs so desirable. The sharing of parameters facilitates the efficient acquisition of positive image attributes. CNNs are used in the method as single-sided classifiers. CNNs are trained using an inversely imbalanced data set that includes a large number of images of lung cancer and a small number of images of unaffected cancer in order to build the single-sided classifiers. According to the findings, single-sided classifiers perform well on samples that have cancer but poorly on ones that are unaffected. Using a thresholding in cancer affected likelihood, samples of unaffected photos are categorized into two groups: suspiciously impacted images and clearly unaffected images. Class imbalance learning leads to a decline in classification performance, which this method takes advantage of. As an obvious non-affected lung, a test sample with a probability below a threshold value is filtered out and given a zero probability value. Test samples are referred to as suspected cancer-affected images and moved on to the next phase if their probability value is higher than the threshold value. In the following step, a test data set is subjected to the same techniques once more. Stage (M-1) is reached by repeating the steps. When a suspected cancer-affected image is given over from stage M, a CNN model trained on a balanced data set determines the nodule probability (M-1).

International Journal of Advanced Trends in Engineering and Management (IJATEM)
Vol. 03 (10), October 2024, pp. 16-30

The test procedure and the training procedure are comparable. A single-sided classifier is trained using an inversely imbalanced data set that is taken from a suspicious data set that was given over in the previous step. The single-sided classifier is used to test the remaining data and exclude images that are clearly unaffected. The test samples that made it past the filter are sent on to the following phase. These processes are carried out repeatedly till stage (M-1). A CNN is trained at stage M after a balanced data set is taken from the suspicious data set that was given over from stage (M-1). The training process is carried out via cross-validation. This led to the creation of CNN models that were trained on various datasets and were able to classify the lung imaging collection. The subsequent stage is able to progressively approximate the combinatorial nature of the categorization according to the cascading CNN classifiers.

The Cascaded CNN substitutes a fully connected layer, a softmax layer, and a classification output layer for the network's final three layers. Assign the last completely connected layer a size equal to the number of training data set classes. To train the network more quickly, raise the fully connected layer's learning rate parameters. It sets the learning rate, mini-batch size, and validation data in accordance with the system's GPU specifications in order to train the network. Use the training data to train the network. It uses the optimized network to classify the validation images and computes the classification accuracy in order to test the network's accuracy. For reliable results, the fine-tuning network is further tested on real-time lung image datasets.

3.5 Predicted Performance Matrix

Several basic indicators, such as TP (True Positive), TN (True Negative), FP (False Positive), and FN (False Negative), are considered in the experimental evaluation that follows. TP stands for attack flows that were correctly anticipated, TN for normal flows that were correctly predicted, FP for attack flows that were mistakenly predicted, and FN for normal flows that were incorrectly predicted.

Accuracy

Accuracy is derived as the ratio of accurate predictions to total predictions; a higher accuracy means that the learning model is making more accurate predictions and it is mentioned as

$$Accuracy = \frac{TP+TN}{TP+FP+TN+FN} \tag{15}$$

Precision

The ability to prevent misclassifying negative records as positive; a low rate of false positives is equivalent to a high precision rate. It is the proportion of accurately anticipated attacks to all predicted attacks, represented by

$$Precision = \frac{TP}{TP+FP} \tag{16}$$

International Journal of Advanced Trends in Engineering and Management (IJATEM)
Vol. 03 (10), October 2024, pp. 16-30

Recall

Recall is the proportion of correctly predicted attacks to actual attacks, or true positive rate, and is represented by

$$Recall = \frac{TP}{TP+FN} \tag{17}$$

F1 score

The F1 score is calculated by averaging Precision and Recall, which is represented by

$$F1\ score = \frac{2.(Recall.Precision)}{Recall+Precision} \tag{18}$$

AUC

At various categorization thresholds, the Area under the ROC Curve (AUC) displays Recall against False Positive Rate.

$$FPR = \frac{FP}{FP+TN} \tag{19}$$

The module makes predictions for the categorized datasets and assesses the confusion matrix, accuracy, recall, time, F1 score, and precision. At last, the classification technique's performance is attained.

4 Results and Discussions

Python software is used to implement this classification model for lung cancer prediction. The collection of lung images, which includes benign, malignant, and normal lung images, is used as the input for the prediction algorithm. For processing, the current images are also in grayscale. In Figure 4, the input image dataset illustrates the benign, malignant and normal lung image dataset.

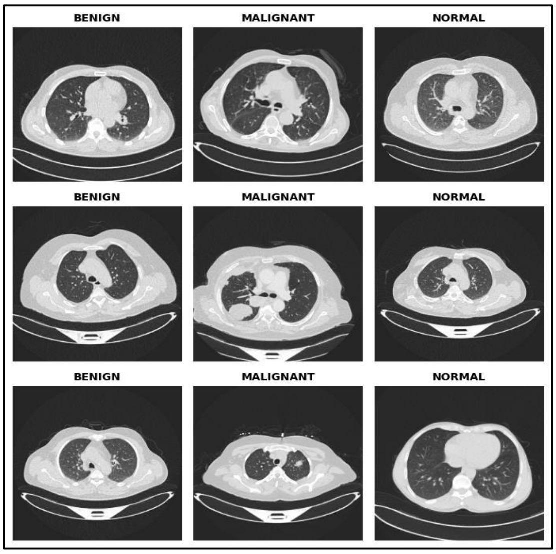

Figure 4: Input image dataset

International Journal of Advanced Trends in Engineering and Management (IJATEM)
Vol. 03 (10), October 2024, pp. 16-30

In Figure 5, the image preprocessing is depicted for the lung image dataset, which contains the cancer affected and non- affected images. After the image is converted into grayscale image for further processing. Each image undergoes preprocessing to get a filtered image using a Weiner filter. The noise removal is calculated using Signal to Noise Ratio (SNR)with value of 0.64 DB, 0.88 DB,0.92 DB, 0.21 DB. Segmentation is employed to segment the lung images using the otsu binary thresholding algorithm. The initial step in segmentation involves normalizing the intensity across the pixel range to effectively differentiate between the cancer affected regions and non-affected regions. The image features are extracted using the LBP algorithm. It encodes the texture information and extract the image features for classification.

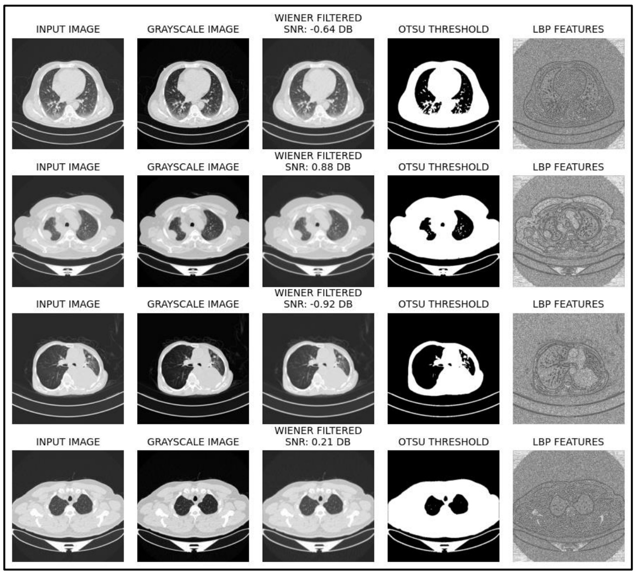

Figure 5: Image dataset after preprocessing, segmentation and feature extraction

A loss metric quantifies the extent of error in a model's prediction for a single sample. A perfect prediction results in a loss value of zero, while imperfect predictions yield higher loss values. From the total number of items in the dataset, accuracy is the percentage of correctly identified cases. The accuracy and loss of the training and validation processes are demonstrated in Figure 6.The accuracy showcasing variations in accuracy to prove the predictive capability of the model. The loss showcasing the variations in loss values, across different examples.

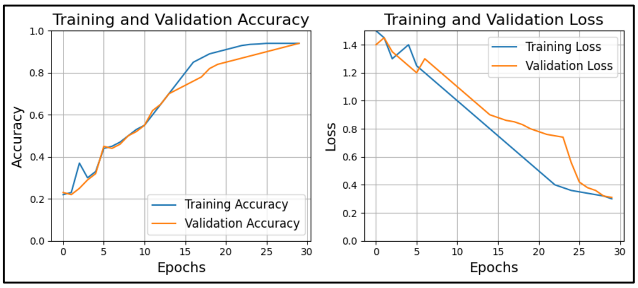

Figure 6: Graphical representation of accuracy and loss in training and validation

ISSN (Online): 2583-7052

International Journal of Advanced Trends in Engineering and Management (IJATEM)
Vol. 03 (10), October 2024, pp. 16-30

Table 1: Performance of Cascaded CNN

Performance	Macro_Averaged Scores	Weighted_Averaged Scores
Precision	0.929	0.933
Recall(Sensitivity)	0.848	0.933
F1 Score	0.878	0.929
Specificity	0.675	_

In Table 1, the performance matrix of the Cascaded CNN is depicted. Cascading classifiers allow the next phase to progressively become closer to the classification's combinatorial nature, It leverages depthwise convolutions to substantially decrease the number of parameters in comparison to other networks, thereby creating a lightweight convolutional neural network. Figure 7 illustrates the confusion matrix. This table compares the actual class (so it is horizontal) with the predicted class (typically vertical).The values for the actual and predicted labels are displayed in this matrix. The effectiveness of classification models, especially those charged with forecasting categorical labels for input examples like normal, benign, and malignant, is frequently assessed using confusion matrices.

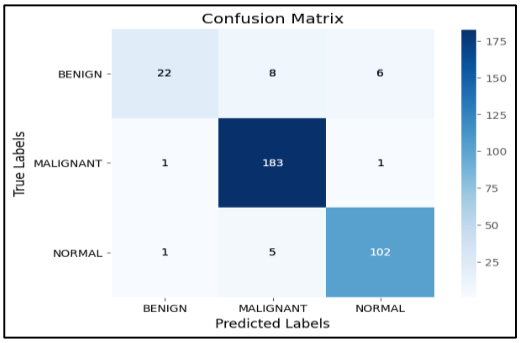

Figure 7: Confusion Matrix

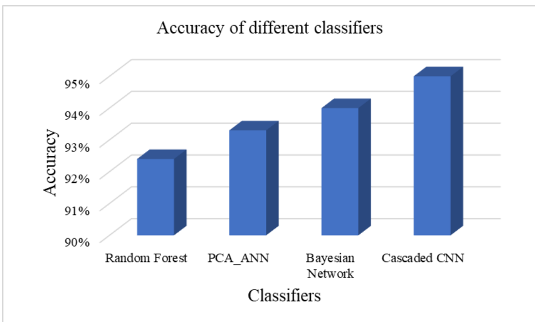

Figure 8: Comparison graph for Accuracy

The accuracy of several classifiers is displayed in Figure 8, with the suggested classifier outperforming other neural network classifiers including Random Forest [3], Principle Component Analysis Artificial Neural Network (PCA-ANN) [5], and Bayesian Network [7] with the maximum accuracy of 95%.

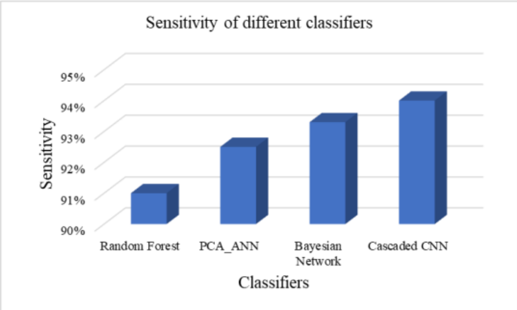

Figure 9: Comparison graph for Sensitivity

Figure 9 shows the sensitivity of various classifiers in which the proposed classifier shows the highest sensitivity of 94% over other neural network classifiers such as Random Forest [3] Principle Component Analysis Artificial Neural Network (PCA-ANN) [5] and Bayesian Network [7].

5 Conclusion

The proposed Cascaded CNN classifier predict the cancer affected lung images from the lung image dataset very efficiently and accurately. In order to improve treatment, this prediction algorithm assists medical professionals in predicting lung cancer using the lung imaging dataset. The results demonstrate that the suggested approach outperforms the current methods in terms of SNR values and offers more information about the image damaged by cancer. The suggested method performs better in terms of F1-score, accuracy, and precision. Notably, the detection rate achieves an impressive F1-score of 93%, specificity of 95%, and sensitivity of 94%. Cascaded CNN significantly improves overall prediction accuracy, achieving a peak accuracy of 95%. In the future, the suggested model may be applied to forecast various chronic illnesses in the medical field and other associated fields.

References

1. Huan-Yu Chen; Hui-Min Wang; Ching-Heng Lin; Rob Yang; Chi-Chun Lee; Year:2023, “Lung Cancer Prediction Using Electronic Claims Records: A Transformer-Based Approach,” IEEE Access, Vol:27, pp. 6062-6073.

2.Ling Chen; Kanfeng Liu; Hui Shen; Hongwei Ye; Huafeng Liu; Lijuan Yu, Year:2021, “Multimodality Attention-Guided 3-D Detection of Nonsmall Cell Lung Cancer in ^{18}F-FDG PET/CT Images,” IEEE Access, Vol: 6, pp. 421-432.

International Journal of Advanced Trends in Engineering and Management (IJATEM)
Vol. 03 (10), October 2024, pp. 16-30

3. Mattakoyya Aharonu; Lokeshkumar Ramasamy, Year: 2024, "A Multi-Model Deep Learning Framework and Algorithms for Survival Rate Prediction of Lung Cancer Subtypes With Region of Interest Using Histopathology Imagery," IEEE Access, Vol: 12, pp. 155309-155329.

4. Pushkar Sathe; Alka Mahajan; Deepak Patkar; Mitusha Verma; Year: 2024, "End-to-End Fully Automated Lung Cancer Screening System," IEEE Access, Vol: 12, pp. 108515-108532.

5. Huitao Qi; Shuangbo Xie; Yanli Chen; Chengqian Wang; Tingting Wang; Bin Sun, Year: 2022, "Prediction Methods of Common Cancers in China Using PCA-ANN and DBN-ELM-BP," IEEE Access, Vol: 10, pp. 113397-113409.

6. Peng Liu; Kexin Jin; Yiping Jiao; Mutian He; Shumin Fei, Year: 2021, "Prediction of Second Primary Lung Cancer Patient's Survivability Based on Improved Eigenvector Centrality-Based Feature Selection," IEEE Access, Vol: 9, pp. 55663-55672.

7. Jinpeng Li; Yaling Tao; Ting Cai, Year: 2021, "Predicting Lung Cancers Using Epidemiological Data: A Generative-Discriminative Framework," IEEE Access, Vol: 8, pp. 1067-1078.

8. Yoganand Balagurunathan; Andrew Beers; Michael Mcnitt-Gray; Lubomir Hadjiiski; Sandy Napel; Dmitry Goldgof, Year: 2021, "Lung Nodule Malignancy Prediction in Sequential CT Scans: Summary of ISBI 2018 Challenge," IEEE Access, Vol: 40, pp. 3748-3761.

9. Rizwan Qureshi; Bin Zou; Tanvir Alam; Jia Wu; Victor H. F. Lee; Hong Yan, Year: 2022, "Computational Methods for the Analysis and Prediction of EGFR-Mutated Lung Cancer Drug Resistance: Recent Advances in Drug Design, Challenges and Future Prospects," IEEE Access, Vol: 20, pp. 238-255.

10. Rahimi Zahari; Julie Cox; Boguslaw Obara, Year: 2024, "Mitigating Diagnostic Errors in Lung Cancer Classification: A Multi-Eyes Principle to Uncertainty Quantification," IEEE Access, Vol: 28, pp. 6828-6839.

11. Francisco Silva; Tania Pereira; Joana Morgado; Julieta Frade; José Mendes; Cláudia Freitas, Year: 2021, "EGFR Assessment in Lung Cancer CT Images: Analysis of Local and Holistic Regions of Interest Using Deep Unsupervised Transfer Learning," IEEE Access, Vol: 9, pp. 58667-58676.

12. Saransh Gupta; Haswanth Vundavilli; Rodolfo S. Allendes Osorio; Mari N. Itoh; Attayeb Mohsen; Aniruddha Datta, Year: 2022, "Integrative Network Modeling Highlights the Crucial Roles of Rho-GDI Signaling Pathway in the Progression of non-Small Cell Lung Cancer," IEEE Access, Vol: 26, pp. 4785-4793.

13. Zehui Liao; Yutong Xie; Shishuai Hu; Yong Xia, Year: 2022, "Learning From Ambiguous Labels for Lung Nodule Malignancy Prediction," IEEE Access, Vol: 41, pp. 1874-1884.

International Journal of Advanced Trends in Engineering and Management (IJATEM)
Vol. 03 (10), October 2024, pp. 16-30

14. Joel Ryan A. de Guzman1; Robert G. de Luna Marife A. Rosales, Year: 2024, "Wiener Filter with Convolutional Neural Network for Noise Removal in API-Based AI Models," ECTI Transactions on Computer and Information Technology, Vol: 18, pp. 456-468.

15. Mohammad A. Alzubaidi; Mwaffaq Otoom; Hamza Jaradat, Year: 2021, "Comprehensive and Comparative Global and Local Feature Extraction Framework for Lung Cancer Detection Using CT scan Images," IEEE Access, Vol: 9, pp. 158140-158154.

16. Mahmoud Ragab; Iyad Katib; Sanaa Abdullah Sharaf; Fatmah Yousef Assiri; Diaa Hamed; Abdullah Al-Malaise Al-Ghamdi, Year: 2023, "Self-Upgraded Cat Mouse Optimizer With Machine Learning Driven Lung Cancer Classification on Computed Tomography Imaging," IEEE Access, Vol: 11, pp. 107972-107981.

17. Vani Rajasekar; M. P. Rangaraaj; S. Vaishnnave, Premkumar; Velliangiri Sarveshwara, Year: 2023, "Lung cancer disease prediction with CT scan and histopathological images feature analysis using deep learning techniques," Vol: 18, pp. 1-18.

18. Tehnan I. A. Mohamed; Absalom El-Shamir Ezugwu, Year: 2024, "Enhancing Lung Cancer Classification and Prediction with Deep Learning and Multi-Omics Data," IEEE Access, Vol: 12, pp. 59880-59882.

19. Rabbia Mahum; Abdulmalik S; Al-Salman, Year: 2023, "Lung-RetinaNet: Lung Cancer Detection Using a RetinaNet with Multi-Scale Feature Fusion and Context Module," IEEE Access, Vol: 11, pp. 53850-53861.

20. Muhammad Imran; Bushra Haq; Ersin Elbasi; Ahmet E. Topcu; Wei Shao, Year: 2024, "Transformer-Based Hierarchical Model for Non-Small Cell Lung Cancer Detection and Classification," IEEE Access, Vol: 12, pp. 145920-145933.